Scanning near-field optical microscopy in Basel, Rüschlikon, and Zürich

Harry Heinzelmann
Thomas Huser
Thilo Lacoste
Hans-Joachim Güntherodt
University of Basel
Institute of Physics
Klingelbergstr. 82
CH-4056 Basel, Switzerland
E-mail: heinzelmann@ubaclu.unibas.ch

Dieter W. Pohl
Bert Hecht
IBM Research Division
Zürich Research Laboratory
Säumerstr. 4
CH-8803 Rüschlikon, Switzerland

Lukas Novotny
Olivier J. F. Martin
Christian V. Hafner
Heinrich Baggenstos
Swiss Federal Institute of Technology
Institute for Field Theory and
High Frequency Electronics
ETH-Zentrum
CH-8092 Zürich, Switzerland

Urs P. Wild, MEMBER SPIE
Alois Renn
Swiss Federal Institute of Technology
Laboratory of Physical Chemistry
ETH-Zentrum
CH-8092 Zürich, Switzerland

Abstract. The concepts of near-field optical microscopy and experimental and theoretical work carried out in Switzerland over the last 10 years are reviewed. After a description of the pioneering experiments of the mid-1980s, we focus on the recent efforts of the three Swiss laboratories currently working in the field in close collaboration. This newly refreshed initiative in near-field optics is supported by the Swiss Priority Program Optique.

Subject terms: scanning near-field optical microscopy; photon-scanning tunneling microscopy; evanescence; shear force imaging; multiple multipole method; light confinement; fluorescence; single-molecule spectroscopy.

Optical Engineering 34(8), 2441–2454 (August 1995).

1 Introduction

Light microscopy was first demonstrated in the late sixteenth century, and has matured into an important technique for routine and exploratory applications in such diverse fields as biology, medicine, and materials sciences. The wealth of optical investigation guarantees conventional light microscopy a place at the side of the higher resolving electron microscopy (EM) and the more recently developed scanning tunneling microscopy (STM) and scanning force microscopy (SFM). Under ideal operating conditions, these techniques enable imaging of atomic surface structures to some extent, but at the expense of the richness of obtainable sample information. The combination of optical microscopy and spectroscopy with resolution comparable to that of EM is an old dream, but progress in classical optical microscopy led only to an asymptotic approach to the diffraction limit, i.e., resolution in the $\lambda/2$ regime.

The only way to further confine optical radiation—a prerequisite for higher resolution—is by material structures with correspondingly small dimensions. Although proposed several times before in this century, only in the early 1980s was this idea converted into an operable microscope, a development that actually had its origin in Switzerland.[1] In the first experiments, a "super-resolution" of 20 to 50 nm was achieved in transmission,[2,3] followed a little later by similar results obtained in reflection.[4] Almost simultaneously, similar work was carried out in the United States.[5]

Paper SWI-65 received Nov. 15, 1995; revised manuscript received Jan. 31, 1995; accepted for publication Feb. 17, 1995.

The new technique, now known as scanning near-field optical microscopy[6–9] (SNOM*) relies on the confinement of optical excitation by tiny apertures, small particles, or pointed tips acting as scattering centers. For selective interaction, these optical probes must be positioned and scanned in immediate proximity to the sample surface, similar to STM or SFM tips. The distance must be kept small such that the evanescent waves around the characteristic structures of probe and sample can overlap to a significant degree.

The most popular optical probes are light-guiding structures that, at one end, force the light through a microscopic aperture with the smallest possible diameter (Fig. 1). At the same time, the light throughput must be maximized. These criteria being counteractive, technical implementations must compromise between resolution and minimum detectable light level.

At resolutions of 100 nm and below, all the relevant interactions are of near-field optical (NFO) type and thus require a treatment that goes beyond the laws of classical optics. NFO knowledge is therefore instrumental for further improvement of resolution, for proper image interpretation, and for applications.

Research in SNOM therefore requires the development, characterization, and control of suitable miniaturized optical tools, on the one hand, and improvements in the understanding of NFO phenomena, on the other. SNOM will be advantageously applied to surfaces where material contrast with a resolution of 10 to 100 nm is of major importance, e.g., in biology or microelectronics. The choice of sample environment is only slightly restricted, enabling SNOM imaging in air, water, vacuum, or at He temperatures.

In Switzerland, research in these areas is pursued in close mutual cooperation. Presently, those are the IBM Research Laboratory in Rüschlikon, the Institute of Physics at the University of Basel, and the Laboratory for Electromagnetic Fields and High Frequency Electronics and the Laboratory of Physical Chemistry of the Swiss Federal Institute of Technology (ETH) in Zürich. Most of these activities are described here. Some further work performed in Basel will be discussed in a separate article.[10]

2 NFO Concepts, Experiments, and Theory

The most popular NFO microscope to date is the aperture SNOM, which is based on the original "Swiss" design[1] (Fig. 2). The optical probe is a pointed transparent tip coated with an opaque metal film in such a way that a small aperture is formed at the apex. In the so-called emission mode, light is coupled into the far end of the probe and guided to the aperture. The tiny transmitted fraction interacts with the object structure in immediate proximity, and is collected by focusing optics, usually a conventional microscope objective.

In general, an auxiliary mechanism is installed for distance control because the optical signal in forward direction is not a monotonous function of the gap width. Electron tunneling between the probe and the sample, as in STM or detection of interfacial forces such as in atomic force microscopy (AFM), are well suited for this purpose.

*An increasing number of acronyms are used in the field, more often than not describing the same concepts. Throughout this paper and following the SXM terminology, we will use the terms SNOM for scanning near-field optical microscopy in general (which is alternatively called NSOM) and STOM for scanning tunneling optical microscopy (which is also called PSTM and EFOM).

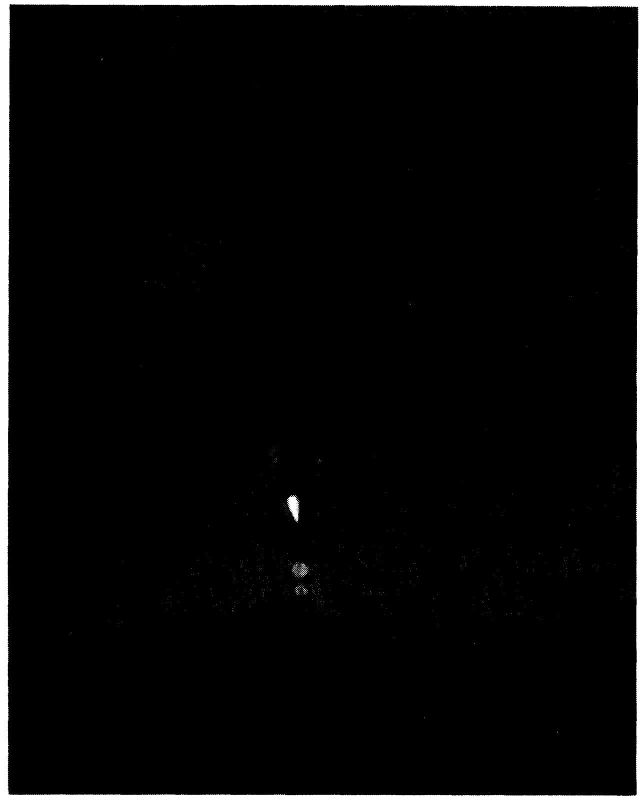

Fig. 1 SNOM fiber probe approaching a test sample surface.

2.1 *Early Work (1983 to 1989)*

From its first demonstration in 1983 until the late 1980s, work on NFO microscopy has been carried out at a few laboratories only. Among these were, besides the IBM Rüschlikon laboratory, Cornell University[5] and the Max-Planck Institute for Biophysical Chemistry in Göttingen, Germany.[11] The activities in Rüschlikon are briefly reviewed here.

2.1.1 *Transmission SNOM*

In the original instrument,[1–3] the optical probe was a quartz crystal, which was cut, polished, and etched in such a way that three facets formed, in principle, an atomically sharp point. The crystal was coated completely with an opaque aluminum film except for the light entrance face opposite the tip [Fig. 2(b)]. The aperture was created by pressing the tip against the sample, causing plastic deformation of the coating until faint transmission of light from the tip could be detected. These optical probes had a large apex angle, which is essential for efficient light throughput, and extremely small apertures; their resolution indeed appears to be unsurpassed. They were somewhat difficult to prepare, however, and fairly short-lived.

The experimental gap width dependence of the transmitted flux is shown in Fig. 2(c) for a metallized sample surface. The flux undergoes a series of interference undulations as the tip is approached to the surface, caused by the light reflected back and forth by the sample surface and the flat end of the tip. The transmission at the end point of this curve (tunnel contact) depends on the value of the dielectric constant of the sample surface. This is the basis of contrast formation in SNOM imaging.

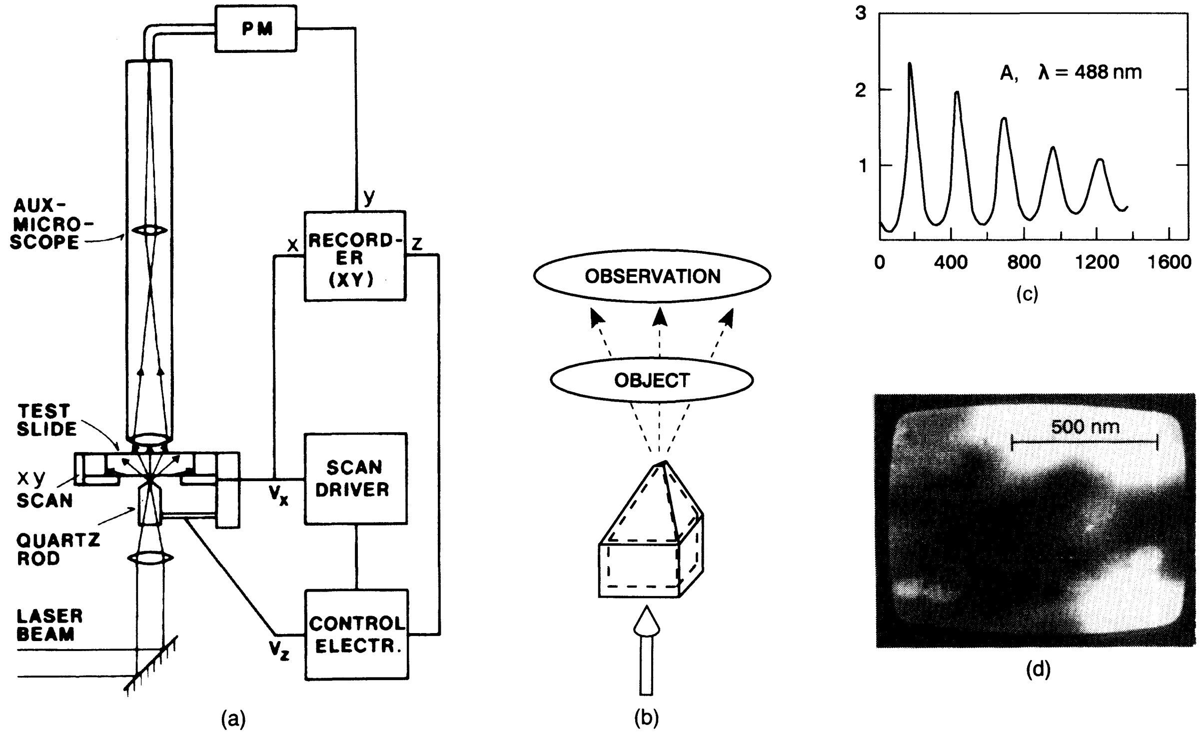

Fig. 2 The original Swiss SNOM: (a) setup (b) scheme of quartz probe tip, (c) approach curves (horizontal axis in nanometers), and (d) SNOM image of metal pattern enables recognition of details of ~20 nm diameter. (From Ref. 3.)

Figure 2(d) shows an image obtained with this type of SNOM. The object is a semitransparent Ta film with holes of 100 nm diameter. The holes are shadow images of latex spheres randomly dispersed on the glass substrate during evaporation. They are clearly visible, together with even smaller details, for instance the ~20-nm-wide peninsula protruding into the pair of holes near the lower right-hand corner. Note that the image is a simple screen shot, because digital image processing was not yet available to us at the time the image was made.

2.1.2 *Reflection SNOM*

The optical probe sketched in Fig. 3 was developed for operation in reflection. It is a section of a planar optical waveguide, which is placed close to the surface. Light scattered by imperfections such as the hole in Fig. 3(b) is the only light observed in the far field—it is essentially a dark-field scheme.[4] The scattering intensity in upward direction depends on the proximity of the sample surface [Fig. 3(c)]. It is possible, in particular, to excite a localized plasmon if the aperture is replaced by a protrusion at a certain small gap width; the particle brightly shines up under these conditions[12] [narrow peak in the approach curve shown in the inset of Fig. 3(c)]. An image obtained with the probe of Fig. 3(b) is shown in Fig. 3(d). A drawback of the method is its restriction to planar or convex samples.

2.2 *Recent Work (Since 1992)*

Since 1992 a wave of interest has stimulated activities in SNOM all over the world. This was triggered in part by the development of more efficient and reproducible optical probes, namely, the metal-coated optical fiber tip[13] and a reliable tip sample distance control based on "shear force" detection.[14,15] In Switzerland, the recently created Swiss Priority Program Optique has been supporting NFO activities since its beginning in 1993.

2.2.1 *"Forbidden light" SNOM*

Besides aperture SNOM, implementations based on tapping an evanescent wave with an uncoated transparent tip have become popular. The principle of operation is strongly analogous to that of the electron STM; this arrangement is therefore known[16–18] as the scanning tunneling optical microscope (STOM) or photon STM (PSTM). In STOM an evanescent field is generated by total internal reflection at the sample surface. This evanescent field is modified by the subwavelength surface topography and by local variations of the index of refraction of the sample. The most popular choice is a sharpened optical fiber as near-field probe. The fiber tip scatters the evanescent field, thereby reemitting a field that propagates in the fiber and that can be detected with conventional means in the far field. The scattered intensity increases exponentially with decreasing tip to sample separation. This is an advantageous feature because high-resolution probe microscopy requires strong gap width dependence of the signal. The image interpretation, however, turns out to be more complicated than that of aperture SNOM.

To combine the advantages of aperture SNOM and STOM, we recently developed a new type of SNOM [Fig. 4(a)], which employs an aperture-type fiber probe, but detects the

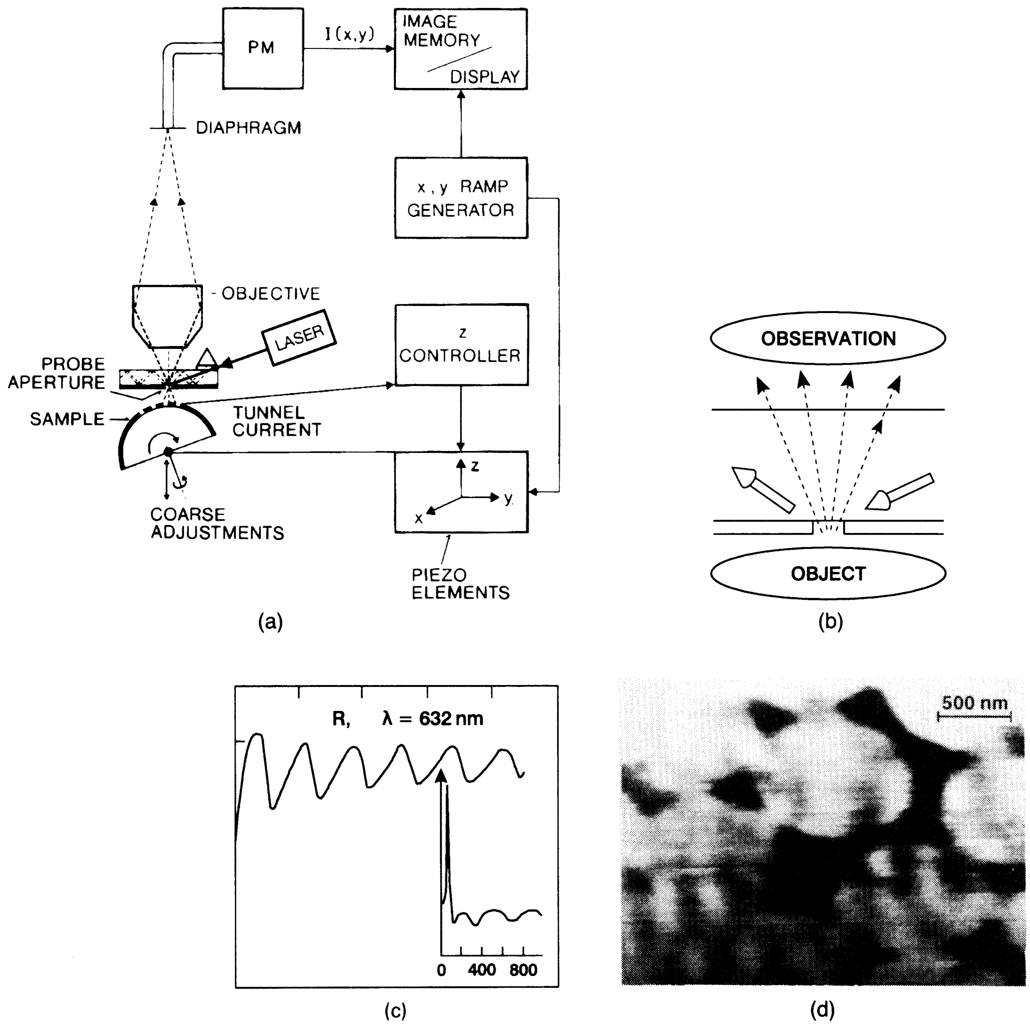

Fig. 3 (a) Setup of reflection SNOM, (b) scheme of aperture dark-field arrangement, (c) approach curves for reflection and plasmon excitation, and (d) image of metal pattern. (From Ref. 4.)

light coupled via evanescent waves (photon tunneling) into the object if the gap width is smaller than approximately one wavelength.[19,20] These contributions are transmitted at angles larger than the critical one and therefore cannot be seen with a regular aperture SNOM; they require an object carrier of, e.g., hemispherical shape. The gap-width-dependent transmission [Fig. 4(b), curve F] provides distinctly enhanced contrast when compared with the regular aperture SNOM mode [Fig. 4(b), curve A]; moreover, it is suitable for distance regulation.

The optical probe in these experiments was the pointed end of an optical fiber, obtained by heating and pulling. Radii of curvature at the apex of 30 nm can be obtained with appropriate choice of parameters. The fiber end is coated with metal (Al) by evaporation from the side while the fiber is being rotated, resulting in an opaque structure with an uncoated spot at the apex of 30 to 100 nm in diameter, which serves as the aperture.

Although the tip-sample distance can be regulated via the intensity of the "forbidden" light, it is advantageous to use nonoptical distance regulation because topographic and optical information can then be decoupled. For this purpose, the standard shear force technique[14,15] (SFT) is used, implemented with an interferometric deflection sensor [Fig. 4(a), inset], as formerly developed[21] for SFM.

Distance regulation by SFT is based on the excitation of a lateral (sideways) vibration of the optical probe tip and the reduction of amplitude when mechanical contact is made. The vibrational motion of the tip usually is determined by optical means, most commonly by knife-edge shadow modulation techniques. To our experience, amplitudes of about 20 nm peak-to-peak are required for the purpose of reliable distance regulation. Because this is too large for high-resolution work, an alternative interferometric detection scheme has been developed: The optical probe fiber is attached near its pointed end to a small piezoelectric bimorph element, which in turn is mounted on top of a standard piezoelectric scanner tube. An ac voltage applied to the bimorph makes it possible to shake the optical probe tip at its mechanical resonance (bending mode, typically 10 to 20 kHz). Also mounted on top is the end of a second fiber, which is part of a four-ended fiber coupler.

The optical probe fiber is illuminated from the side through the coupler fiber with the light from an IR diode laser. Interference between light reflected from the metallized wall of the probe fiber and the end face of the coupler fiber creates

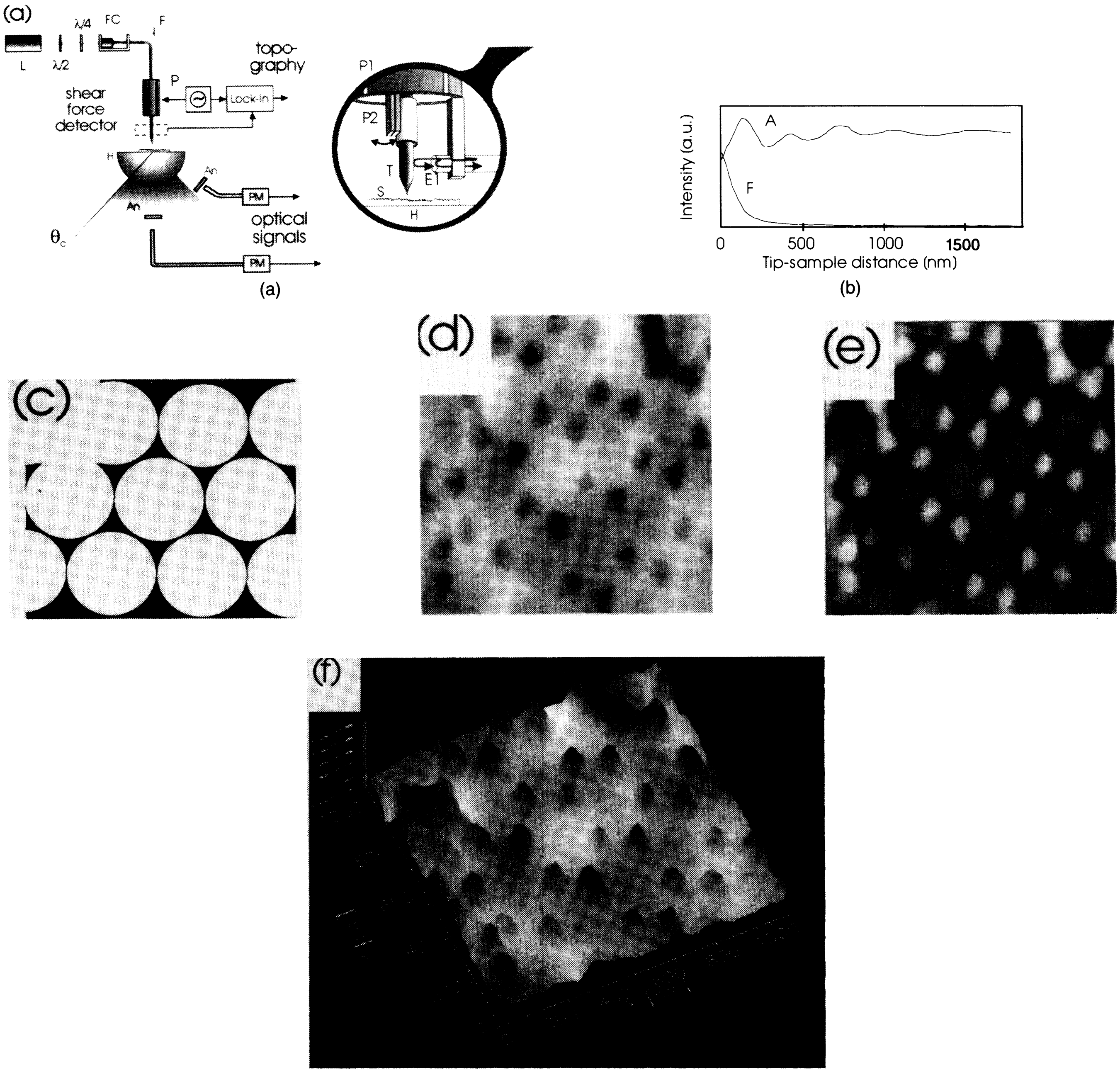

Fig. 4 "Forbidden" (and "allowed") light SNOM (Refs. 19 and 20): (a) setup, inset; detail showing interferometric shear force sensor and (b) approach curves (A is allowed light, F is forbidden light). Imaging 50-nm-sized objects with green light (wavelength 515 nm) and the "forbidden light" SNOM: the object, shown schematically in (c), is a latex sphere shadow mask; the shadow mask of a latex sphere lattice, tiny metal patches of nearly triangular shape arranged in an almost perfect hexagonal array. These show up as dark spots in the optical image (d), as bright spots in the friction/topography signal (e), and as elevations in the superposition of (d) and (e), shown in (f). These spots are the residuals from a thin metal film, which was evaporated on a latex sphere lattice. The latter was obtained by depositing commercially available latex spheres with radius $r = 110$ nm on a glass substrate. After evaporation, the spheres were washed away, leaving only the metallized interstices on the glass slide. The equilateral triangle drawn into such an interstice has a height of $\approx$50 nm. (The object was kindly supplied by U. Ch. Fischer, University of Münster.)

a modulated signal. As soon as the tip of the probe gets into mechanical contact with the object surface, frictional forces begin to damp the oscillation. A control circuit fed by the interference signal and acting on the scanner piezo tube enables operation of the system at constantly reduced amplitude, like a standard SFM. The interferometric force distance control can be operated with excitation amplitudes of 2 nm peak-to-peak and less. SNOM with SFT thus provides topographic images of reasonable quality together with the optical scan images. Simultaneously obtained optical and shear force im-

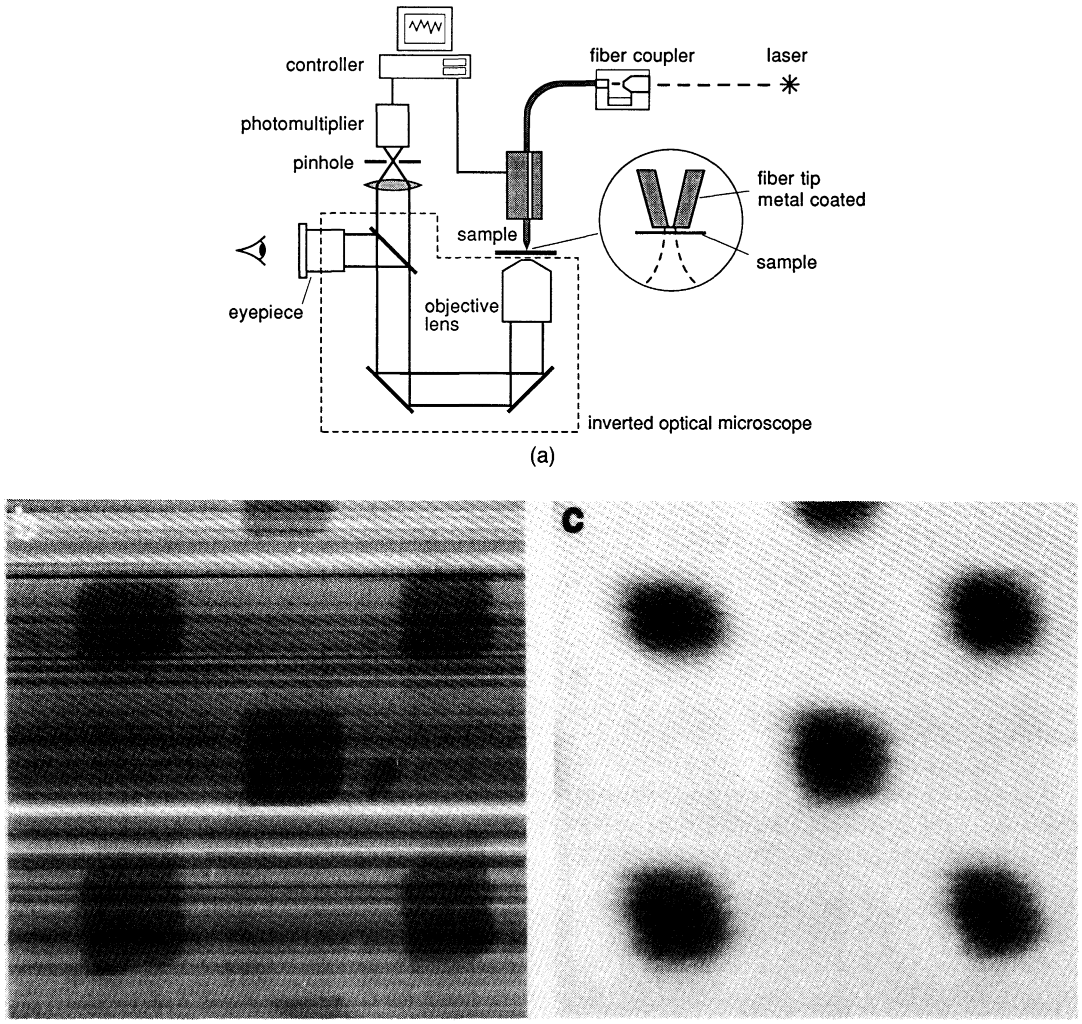

Fig. 5 SNOM combined with a conventional optical microscope. Setup (a) and images of a Cr pattern on a glass substrate (b) unprocessed constant shear force image; because of contrast reversal, the Cr patches are observed as dark areas (c) SNOM signal in transmission; the Cr patches appear dark because of higher absorption (the intensity range is 0.5 nW). (From Ref. 22.)

ages of an object are shown in Figs. 4(d) through 4(f). The object is a latex sphere shadow mask sketched schematically in Fig. 4(c).

2.2.2 *"Workhorse" SNOM for imaging*

The development of two other near-field optical microscopes has been pursued recently.[22] One is a conventional aperture-type SNOM placed on top of the sample stage of an inverted optical microscope [Fig. 5(a)]. It enables conventional optical previewing and zooming in on interesting sample locations for subsequent SNOM imaging, combined with fluorescence and polarization contrast already implemented in the optical microscope. This makes the setup best suited for imaging inhomogeneous surfaces, e.g., biological samples.

In addition to the conventional and NFO microscopes, we implemented shear force detection, enabling concurrent topographic imaging of the sample surface (see description earlier). The fiber motion is recorded by a 670-nm laser diode projecting the shadow image of the tip onto a photo detector.

Figures 5(b) and 5(c) show images acquired by this instrument on a test sample made from ~15-nm-high and 0.5-μm-wide Cr squares patterned in a checkerboard fashion onto a glass substrate. Topography [Fig. 5(b)] and near-field optical signal in transmission [Fig. 5(c)] were acquired simultaneously. Because of contrast reversal, which is sometimes observed in shear force imaging, the Cr squares appear as dark depressions in the topography, as opposed to protrusions. This effect is likely caused by strongly varying adhesive interactions when scanning the tip across glass/Cr boundaries. In the optical image, the Cr squares appear dark, because of larger absorption of the metal.

2.2.3 *Combined optical tunneling/force microscope*

A new development is the combination of an STOM and an SFM. The tip of the SFM cantilever acts as a scattering center that disturbs the evanescent field above the sample[23,24] in much the same way as the described bare optical fiber tip. This process generates propagating waves that can be detected in the far field. The distance regulation between tip and sample in contact-mode AFM is straightforward in this arrangement. In this scheme, the resolution is not determined by the smallness of optical apertures, which is limited by the

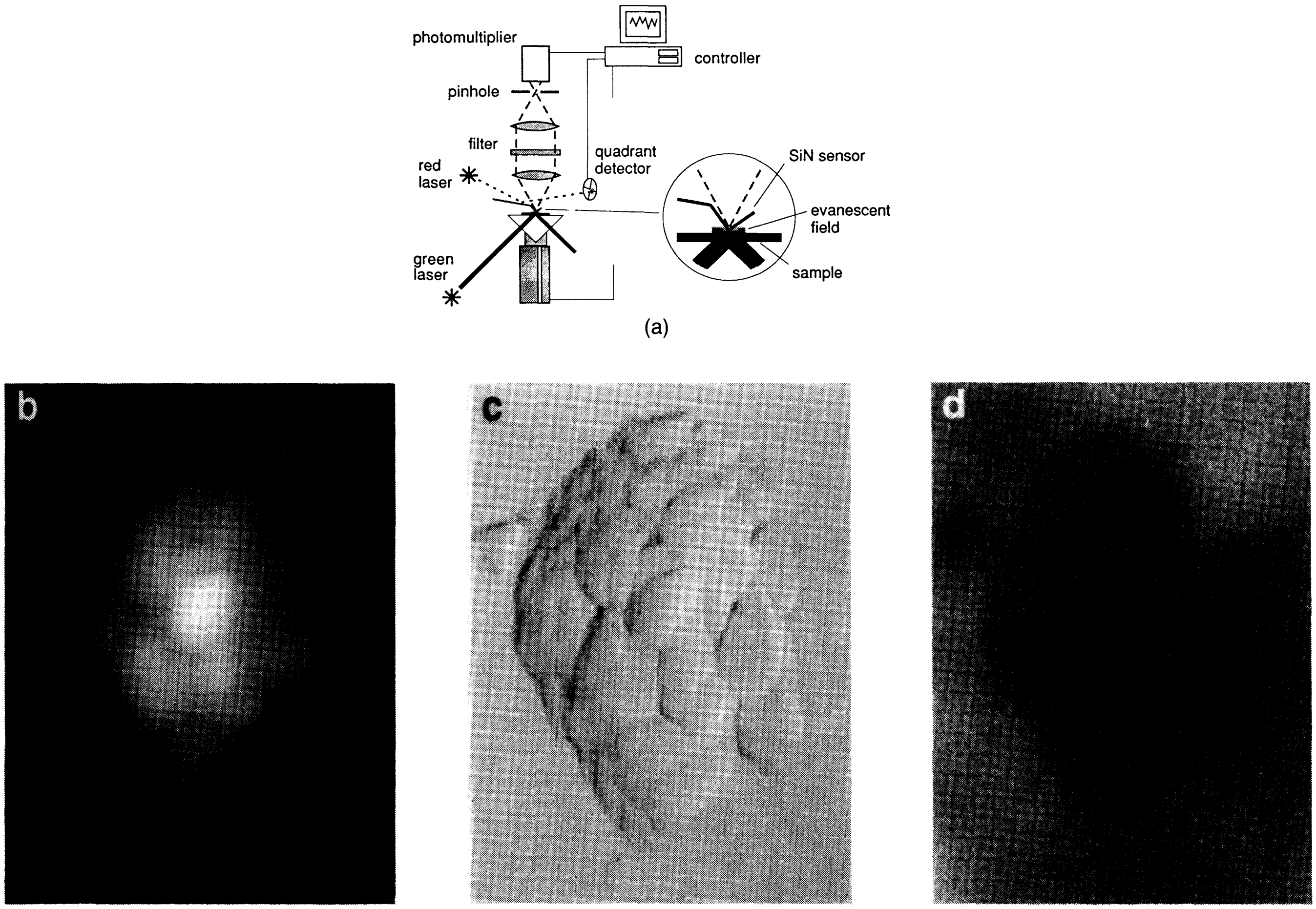

Fig. 6 STOM combined with a force microscope: setup (a) and 0.88×1.33 μm^2 scan of a grain on a glass surface of (b) topography, (c) lateral force, and (d) light intensity. The images were taken simultaneously. (From Ref. 22.)

penetration depth of the metal coating. Rather, as a scattering scheme, it carries the potential for higher spatial resolution, because even a single atom can act as a scattering center. Additionally, it can be speculated that a pyramid cone with a large opening angle, which is most common as force microscope probe tip, is a more efficient light collector than the overdamped waveguide structure of a tapered fiber tip. To aid the interpretation of the optical data, it is a great advantage to simultaneously acquire a force topograph of the sample surface.

The schematic arrangement is shown in Fig. 6(a). A glass prism is mounted on a *xyz* piezoscanner. The transparent sample is placed on the prism surface and optically contacted by index-matching oil. Light from a green HeNe laser ($\lambda = 543.5$ nm) undergoes total internal reflection inside the prism and generates an evanescent field above the sample. The metal coating of a commercial Si_3N_4 cantilever is stripped off by etching in King's water ($3HCl + HNO_3$) to make them transparent. The light, which is scattered at the tip, passes through the cantilever, is collected by a lens, and is focused through a pinhole onto a photomultiplier tube. The pinhole is used to spatially filter out stray light coming from the surrounding of the tip. The light intensity that reaches the photomultiplier tube is typically 0.25 nW.

The deflection of the cantilever is measured by reflecting a focused laser beam of a laser diode ($\lambda \approx 670$ nm) from the cantilever to a quadrant detector. This arrangement represents the AFM part of the microscope. Normal forces are correlated to the topography of the sample, lateral forces are caused by local friction between tip and sample and result in a torsion of the cantilever. Both components result in a displacement of the reflected beam on the quadrant detector. In this way, it is possible to obtain three different images of the sample simultaneously: topography, friction force, and optical light intensity.

Figure 6(b) shows the image of a particle on a glass surface obtained with the combined STOM/SFM. The scan was made in constant force mode and the scan region was 0.88×1.33 μm^2. The sample topography [Fig. 6(b)] shows a particle height of approximately 92 nm. As can be seen more readily in the lateral force image [Fig. 6(c)], the particle has a detailed fine structure. It is not unusual for force microscopy that the lateral force image shows a significantly better contrast of the surface topography than the one recorded with normal

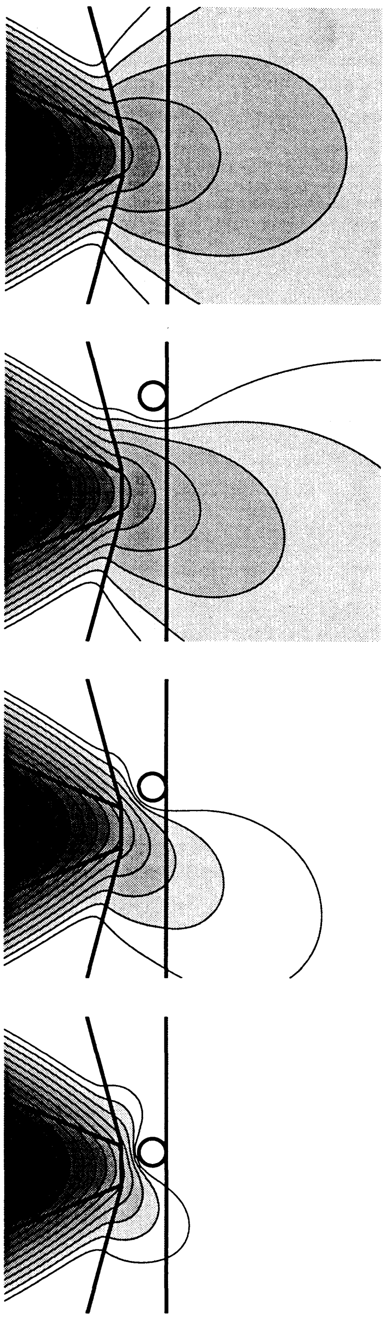

Fig. 7 Scanning a 2-D SNOM probe over a metal particle. Contours of constant $|E|^2$ (factor of 2 between successive lines). The polarization is perpendicular to the plane of the figure (*s* polarization).

force. The surface structure is also observed, with less resolution, in the near-field optical image [Fig. 6(d)]. The highest point of the grain has the least light intensity. The whole picture is superposed by light scattered and diffracted by the grain.

2.2.4 *Theoretical studies of SNOM*

In near-field optics both the classically termed near-field (Fresnel) and far-field (Fraunhofer) regimes are relevant. Furthermore, subwavelength objects as well as large structures are of interest. Therefore, theoretical tools of classical optics such as diffraction theory can be applied in a very limited range only, i.e., as long as edge effects are negligible. As a consequence, the questions of achievable resolution and contrast had been left to heuristic arguments and experimental evidence for a long time. A profound understanding demands for exact solutions of Maxwell's equations. Analytical solutions would be best for theoretical understanding but can be obtained for simple problems only.

The multiple multipole method[25] (MMP) used in most of our theoretical investigations is an efficient compromise between analytical and numerical approaches: Only the boundaries between the individual homogeneous domains are discretized; the fields within the domains are described by analytical solutions of Maxwell's equations.

The theoretical investigations started with 2-D models.[26] Figure 7 shows a metallic particle, which is scanned with an aperture-type SNOM. The optical probe consists of a truncated glass wedge embedded in an aluminum screen such that a narrow slit is formed at the bottom face. The light emitted by the slit illuminates the metal particle, which sits on a dielectric substrate. The light also penetrates into the aluminum screen where a considerable amount of the power is dissipated (skin depth = 6.5 nm). The polarization was chosen to be perpendicular to the plane of the figure (*s* polarization). The metal particle acts like a mirror in this case. When located at center position the radiation from the aperture is decreased. A far-field detector hence registers a negative dip when the particle is scanned. The situation is different when scanning over a dielectric particle. The field is attracted by the particle leading to an enhanced signal when the particle is close to the aperture. Thus, metallic particles lead to negative contrast, dielectric ones to positive contrast.

Recently, the first 3-D investigations, which require considerable computational effort, were performed.[27] In Fig. 8(a), the field in the foremost region of a conical probe is shown on three perpendicular planes of which ($y=0$) is the plane of polarization. The probe consists of a tapered dielectric core and a tapered aluminum cladding. The field is excited by the analytically known cylindrical HE_{11} waveguide mode[28] incident from above. The field decays very fast (7 orders of magnitude over the whole tapered region) toward the aperture since the diameter of the core is below cutoff.

When the probe is approached toward a dielectric substrate the power flux through the probe increases as shown in Fig. 8(a, right). Therefore, the light source cannot be considered to be independent of its surrounding. Instead, the coupling between source and objects must be taken into account in a self-consistent way. This is a general complication inherent to SNOM, and actually any type of scanning probe microscopy: An image obtained by scanning over a sample never represents only the optical properties and topography of the sample, but also includes the interaction between source and sample. Note that in front of the aperture the field extends over a much larger distance in the *xz* plane ($y=0$) than in the *yz* plane ($x=0$). Furthermore, for $y=0$, the field is enhanced also on the outer edge of the cladding because of the large component of the electric field perpendicular to the boundary and due to the high curvature of the edge (lightning rod effect). It can hence be expected that scanning with different polarization leads to different images.[26]

The field behind the aperture consists of both propagating and evanescent components. As long as no small scale object is present, the latter do not contribute to radiation but oscillate

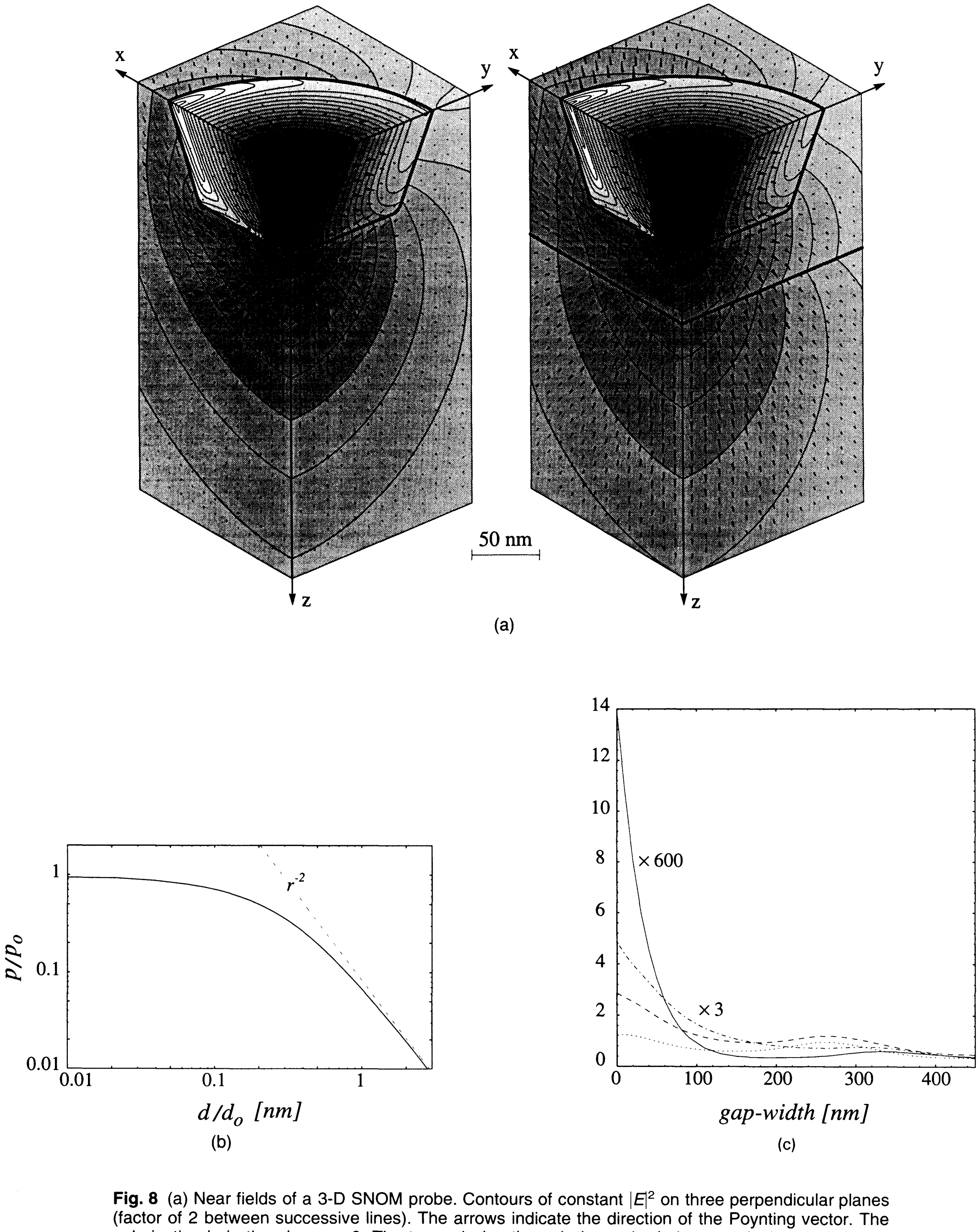

Fig. 8 (a) Near fields of a 3-D SNOM probe. Contours of constant $|E|^2$ on three perpendicular planes (factor of 2 between successive lines). The arrows indicate the direction of the Poynting vector. The polarization is in the plane $y=0$. The transmission through the probe is increased when a dielectric substrate ($\varepsilon_{subs}=2.25$) is approached. (b) Extension of the near field behind the aperture. Normalized power density on a line in forward direction through the center of the aperture. The distance d from the aperture is normalized with the diameter of the aperture d_o. After a distance of half of the aperture diameter, the field already decays with r^{-2}, which is characteristic for far-field behavior. (c) Dependence on gap-width for different signals detected in the far field: total power coupled into the allowed zone (dotted curve), total power radiated into the substrate (dashed curve), total power coupled into the forbidden zone (dash/dotted curve), and power coupled into a lens (angle of acceptance = 10 deg) located in the plane of polarization at $\theta=70$ deg from the forward direction (solid curve). For gap widths smaller than 120 nm, the solid curve decays exponentially with a $1/e$ decay length, which is in agreement with the corresponding decay length of the evanescent field originating from total reflection. (From Ref. 27.)

as reactive power. The evanescent wavelets, which have huge **k** vectors can be converted into propagating ones by structures whose spatial Fourier spectrum has correspondingly large components. Figure 8(b) shows the power density along the z axis behind the aperture. The near-field zone extends over a region that is of the size of half of the aperture diameter. At larger distance the power density decays as r^{-2}, which is characteristic for far-field behavior.

In Fig. 8(c), the probe is approached toward a dielectric substrate and different signals in the far field are detected as a function of the distance between probe and substrate. The dotted curve represents the power radiated into the allowed zone and the dashed curve the total power coupled into the substrate. Both curves are more or less dominated by interference undulations. On the other hand, the power radiated into the forbidden zone (dash/dotted curve) shows a smooth, monotonic decay. The solid curve finally is obtained by detecting the power at an angle of 70 deg from the z axis (angle of acceptance = 10 deg) in the plane of polarization. For probe-substrate distances up to 150 nm, this curve shows an exponential decay with a $1/e$ length, which agrees with the decay length of a corresponding evanescent wave generated by total internal reflection.

As already mentioned, the extraordinary resolution obtained in NFO originates from the fact that a subwavelength structure can confine light. Indeed, such a confined electromagnetic field can perfectly reproduce the structure shape and, if recorded with a NFO probe, produce a high-resolution image of the structure. This is visible in Figs. 9(a) and 9(b), where we report the amplitude of the field scattered by a thin 3-D dielectric object with a "swiss cross" shape. The object is 7.5 nm thick, its dielectric constant is 2.25, and it is sur-

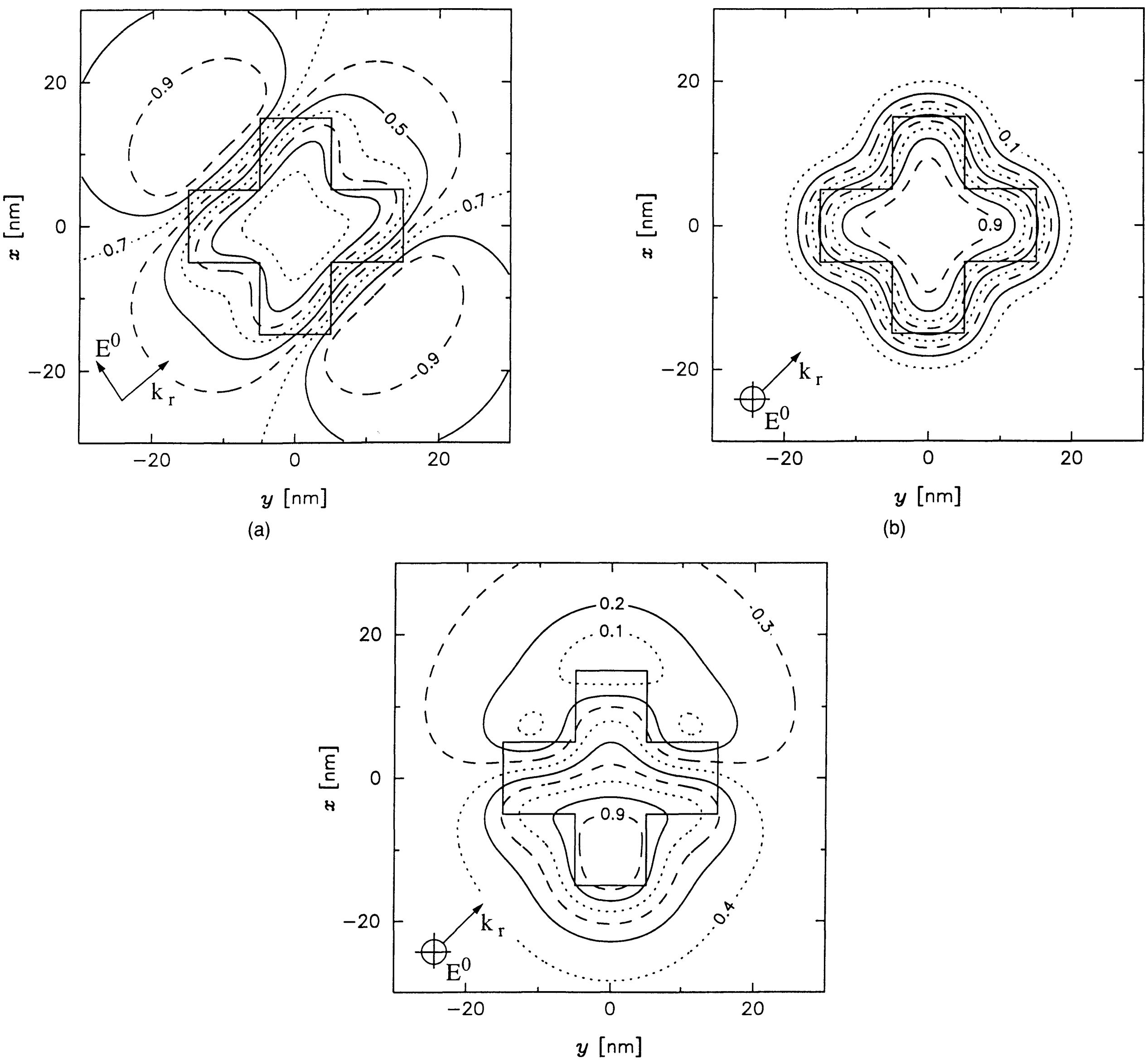

Fig. 9 Field amplitude in an observation plane located 5 nm above the scattering system: (a) TE incident field and (b) TM incident field. The propagation direction $\mathbf{k}_r$ and the polarization of the incident field E^0 are represented in each figure. (c) Same situation as in (b), but for an anisotropic scattering system.

rounded by vacuum. The cross is illuminated from the side with a plane wave E^0 propagating with a wave vector $\mathbf{k}_r$ in the x-y plane; the wavelength is 633 nm. The scattered field is recorded in a plane parallel to the cross, located at a distance of 5 nm above the structure. Two different polarizations are investigated: incident field parallel to the observation plane [transverse electric field (TE), Fig. 9(a)] and incident field orthogonal to the observation plane [transverse magnetic field (TM), Fig. 9(b)].

In the TE case, strong field gradients appear along the object sides that are orthogonal to the incident electric field [Fig. 9(a)]. Thus different sides of the object are enhanced, depending on the orientation of the incident electric field, and the field pattern strongly depends on the propagation direction of the incident field. The field intensity in the detection plane is highest immediately outside the cross and decreases above it, leading to an inverse contrast image of the object. Furthermore, the image does not at all reproduce the cross shape.

For a TM field, the behavior is completely different. Now the isoamplitude lines perfectly follow the contour of the object, although its size is much smaller than the wavelength [Fig. 9(b)]. Furthermore, the image does not depend on the orientation of the incident field, and the field pattern always reproduces the object shape. A strong confinement of the field above the object is also visible. Such a confined field can be recorded by a SNOM probing device, which explains the extraordinary resolution obtained with such a device.

These results were obtained with a new method developed in a joint project between the Institute for Field Theory and High Frequency Electronics at the ETH, Zürich; Institute for Studies in Interface Sciences in Namur, Belgium; and the Centre National de la Recherche Scientifique (CNRS) in Besançon, France. This approach is based on the Green's function technique and has proven to be very well suited for the theoretical investigation[29–32] of NFO. An important advantage of this approach is that it can easily take anisotropic media into account. The study of anisotropic media represents an extremely promising application of NFO, which opens numerous perspectives in rapidly growing research areas such as, for example, magneto-optical data storage.

The phenomena encountered in the study of the interaction of light with anisotropic media are rather complex and the development of theoretical methods able to handle such media is mandatory for guiding and analyzing the forthcoming experimental work. This is illustrated in Fig. 9(c), where we report the field scattered for a similar situation as in Fig. 9b, but with an anisotropic dielectric media. Although some field confinement in the object is still visible in Fig. 9(c), the field pattern is quite distorted and no longer follows the shape of the scattering system. This is the result of the ''off-diagonal'' elements of the dielectric tensor, which couple the different field components together.

2.2.5 *Fluorescence microscopy*

Single molecules with specific photophysical properties have recently been characterized by fluorescence excitation spectroscopy at low temperatures.[33–35] In a suitable host such as a crystal of p-terphenyl a small number of luminescent guest molecules, e.g., pentacene, are excited by very monochromatic light. At a temperature of a few degrees Kelvin the homogeneous linewidth of the molecules approaches the fluorescent lifetime limited value (several megahertz) and is about 1000 times smaller than the inhomogeneous width. Individual molecules can be observed by scanning the optical frequency over several gigahertz. Sensitive detection methods such as photon counting are employed. The number of photons per second detected from a single molecule can reach 100,000. Single molecules are extremely sensitive probes of the environmental conditions: the spectrum of a single molecule, for instance, shifts as a function of external pressure.[36] A pressure change of only 500 hPa (0.5 bar) shifts the single molecule peak by 500 MHz.

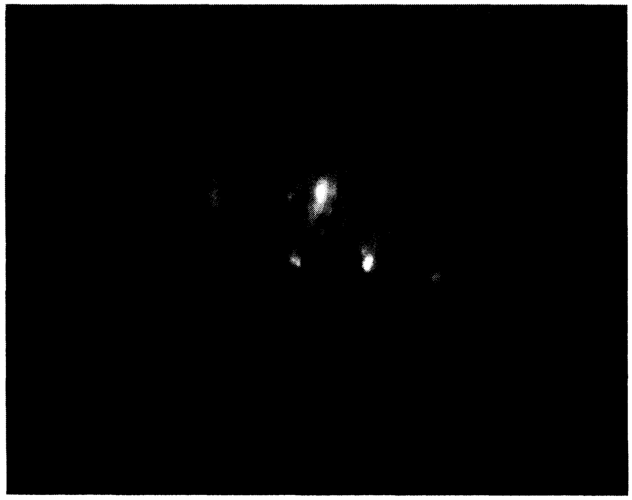

Fig. 10 Fluorescence image of a hexadecane sample containing terrylene molecules. The sample was illuminated at 574.319 nm with 25-μW laser power. The fluorescence light was integrated over 10 s. The diameter of the imaged sample region was estimated to about 100 μm.

Single luminescent molecules have very recently also been observed under a ''conventional'' microscope,[37] which, however, must be operated at a temperature of 2 K. Each molecule represents a point light source and appears as an Airy disk with a diameter of the order of some micrometers determined by the aperture of the microscope. In Fig. 10, one of the first microscopic images of terrylene molecules in hexadecane is shown. In these investigations, the additional parameter ''excitation wavelength'' enables extremely high resolution spectroscopy in the visible spectral range. All of the spectroscopic studies performed earlier, such as Stark effect[35] and pressure effect,[36] are at present under investigation with the ''conventional'' microscope. The main advantage is the parallelism offered by the 2-D image plane. Many ''single'' molecules can be investigated at the same time under identical conditions.

To combine the spectral resolution of ''single molecule'' spectroscopy with the excellent spacial resolution properties of the near-field technique, a SNOM operating at 2 K has been developed.[38] Whereas with shear-force detection it is difficult to control the approach of the tip in superfluid helium, the forbidden light SNOM is excellently suited to single-molecule experiments. In the experiments performed until now, the spectroscopy and not the imaging concepts were stressed. The distance of the molecules from the fiber tip was identified by observing the saturation properties of the emis-

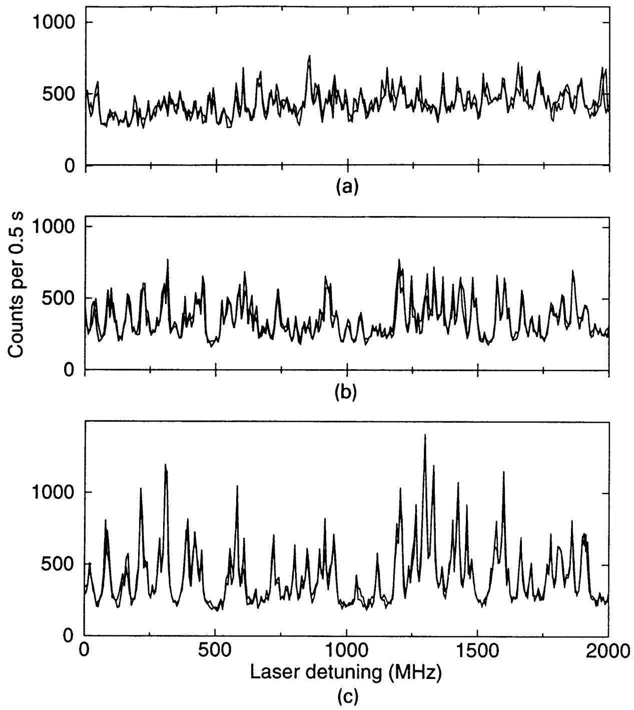

Fig. 11 Statistical fine structure and single-molecule features on approaching the near field region. Approximate distances from the surfaces are (a) 1.2 μm, (b) 0.5 μm, and (c) 210 to 270 nm. Each panel presents two spectra taken approximately 5 min apart to show reproducibility. Zero detuning = 592.066 nm (16,890.0 cm^{-1}).

sion and of the Stark shift of the spectrum with respect to a voltage applied to the fiber tip. Figure 11 shows the changing pattern of the spectrum during a tip approach. At a distance of 1.2 μm between the tip and the sample surface many molecules are excited and a statistical fine structure is seen. At a distance of 210 to 270 nm, the individual signals from the molecules are well resolved, and about 40 molecules can be identified separately.

3 Summary

Near-field optics extends the possibility of optical characterization to nanometer dimensions. Resolution of 30 to 70 nm is the state of the art, and it has been achieved with a number of different implementations (SNOM, STOM, modified AFM). It opens opportunities, in particular with regard to material contrast at high resolution, which is not available with conventional microscopy or with one of the alternative scanning probe microscopies.

Computer-aided design on the basis of the Maxwell/Helmholtz equations provides deeper understanding of the optical processes occurring in nanometer structures.

4 Outlook

Our research activities are directed toward three related goals:

1. demonstration of practical applications using the existing technology
2. characterization of the different types of SNOMs and development of improved instruments
3. pushing the limits of resolution by the development and testing of new concepts and implementations.

Pursuit of these goals requires both experimental and theoretical work. Improved optical probes must be manufactured with nanometer size tolerances and operated with extremely precise control. Computer-aided design on the basis of the Maxwell/Helmholtz equations will provide guidelines for optimized structures for field enhancement and confinement. Such a capability is of interest not only for SNOM but also for other branches of nanoscale science and technology.

Further progress also requires advances in NFO in general, an interesting challenge with regard to principal understanding, the creation of theoretical/mathematical tools with predictive power, and the development of concepts for utilization in science and technology. The "parallel action" of experimental and theoretical efforts in our group is of particular value in this situation.

Acknowledgments

We would like to thank U. Ch. Fischer (University of Münster), M. Fujihira (Tokyo Institute of Technology), and B. Curtis (Paul Scherrer Institute, Villigen) for providing various test samples. The experimental work in Rüschlikon profited significantly from instrumentation made available by the local Optoelectronics Department, which is gratefully acknowledged. Similarly, the Basel experiments were possible only with the help of the local probe microscopy and optics groups. The work has been supported in part by the Swiss Priority Program, Optique, and the Swiss National Science Foundation.

References

1. D. W. Pohl, W. Denk, and M. Lanz, "Optical stethoscopy: image recording with resolution λ/20," *Appl. Phys. Lett.* **44,** 651 (1984).
2. D. W. Pohl, W. Denk, and U. Dürig, "Optical stethoscopy: imaging with λ/20," *Proc. SPIE* **565,** 56 (1985).
3. U. Dürig, D. W. Pohl, and F. Rohner, "Near-field optical-scanning microscopy," *J. Appl. Phys.* **59,** 3318 (1986).
4. U. C. Fischer, U. T. Dürig, and D. W. Pohl, "Near-field optical scanning microscopy in reflection," *Appl. Phys. Lett.* **52,** 249 (1988).
5. A. Lewis, M. Isaacson, A. Harootunian, and A. Murray, "Development of a 500 Å spatial resolution light microscope," *Ultramicroscopy* **13,** 227 (1984).
6. Proceedings of the 2nd Conference on Near-Field Optics, Raleigh, NC, 20–22 October 1993, *Ultramicroscopy,* Vol. 57 (1995).
7. D. W. Pohl, *Advances in Optical and Electron Microscopy,* Vol. 12, 243–312, Academic Press, New York (1991).
8. E. Betzig, J. K. Trautman, T. D. Harris, J. S. Weiner, and R. L. Kostelak, "Breaking the diffraction barrier: optical microscopy on a nanometric scale," *Science* **251,** 1468 (1991).
9. H. Heinzelmann and D. W. Pohl, "Scanning near-field optical microscopy," *Appl. Phys. A* **59,** 89–101 (1994).
10. A. J. Meixner, D. Zeisel, M. A. Bopp, and G. Tarrach, "Super resolution imaging and detection of fluorescence from single molecules by scanning near-field optical microscopy," in this issue.
11. U. C. Fischer, "Optical characteristics of 0.1 μm circular apertures in a metal film as light sources for scanning ultramicroscopy," *J. Vac. Sci. Technol. B* **3,** 386 (1985).
12. U. C. Fischer and D. W. Pohl, "Observation on single-particle plasmons by near-field optical microscopy," *Phys. Rev. Lett.* **62,** 458 (1989).
13. E. Betzig and J. Trautman, "Near-field optics: microscopy, spectroscopy, and surface modification beyond the diffraction limit," *Science* **257,** 189 (1992).
14. R. Toledo-Crow, P. C. Yang, Y. Chen, and M. Vaez-Iravani, "Near-field differential scanning optical microscope with atomic force regulation," *Appl. Phys. Lett.* **60,** 2957 (1992).
15. E. Betzig, P. L. Finn, and S. J. Weiner, "Combined shear force and near-field scanning optical microscopy," *Appl. Phys. Lett.* **60,** 2484 (1992).
16. D. Courjon, K. Sarayeddine, and M. Spajer, "Scanning tunneling optical microscopy," *Opt. Commun.* **71,** 23 (1989).
17. R. C. Reddick, R. J. Warmack, and T. L. Ferrell, "New form of scanning optical microscopy," *Phys. Rev. B* **39,** 767 (1989).
18. N. F. van Hulst, F. B. Segerink, and B. Bölger, "High resolution imaging of dielectric surfaces with an evanescent field optical microscope," *Opt. Commun.* **87,** 212 (1992).

19. B. Hecht, H. Heinzelmann, and D. W. Pohl, "Combined aperture SNOM/PSTM: the best of both worlds?" in *Proc. 2nd Conf. on Near-Field Optics,* Raleigh, NC, 20–22 October 1993, Ultramicroscopy (1994).
20. H. Heinzelmann, B. Hecht, L. Novotny, and D. W. Pohl, "Forbidden light scanning near-field optical microscopy," *J. Microsc.* **177,** 115 (1994).
21. D. Rugar, H. J. Mamin, R. Erlandsson, J. E. Stern, and B. D. Terris, "Microscope using a fiber-optic displacement sensor," *Rev. Sci. Instrum.* **59,** 2337 (1988).
22. T. Lacoste, T. Huser, H. Heinzelmann, and H.-J. Güntherodt, "Near-field optical microscopes for high resolution imaging," in *NATO Series E: "Photons and Local Probes,"* O. Marti and R. Möller, Eds. Kluwer Academic Publishers, Dordrecht (in press).
23. N. F. van Hulst, M. H. P. Moers, O. F. J. Noordman, R. G. Tack, and F. B. Segerink, "Near-field optical microscopy using a silicon-nitride probe," *Appl. Phys. Lett.* **62,** 461 (1993).
24. F. Baida, D. Courjon, and G. Tribillon, "Combination of a fiber and a silicon nitride tip as a bifunctional detector; first results and perspectives," in *Proc. NFO I: "Near Field Optics,"* NATO ASI Series E, Vol. 242, D. W. Pohl and D. Courjon, Eds., p. 71 (1993).
25. C. Hafner, *The Generalized Multiple Multipole Technique for Computational Electromagnetics,* Artech, Boston (1990).
26. L. Novotny, D. W. Pohl, and P. Regli, "Light propagation through nanometer-sized structures: the two-dimensional-aperture scanning near-field optical microscope," *J. Opt. Soc. Am. A* **11,** 1768 (1994).
27. L. Novotny and D. W. Pohl, "Light propagation in scanning-near field optical microscopy," in *NATO Series E: "Photons and Local Probes"* O. Marti and R. Möller, Eds., Kluwer Academic Publishers, Dordrecht (in press).
28. L. Novotny and C. Hafner, "Light propagation in a cylindrical waveguide with a complex, metallic dielectric function," *Phys. Rev. E* (in press).
29. O. J. F. Martin, A. Dereux, and C. Girard, "Iterative scheme for computing exactly the total field propagating in dielectric structures of arbitrary shape," *J. Opt. Soc. Am. A* **11,** 1073 (1994).
30. C. Girard and A. Dereux, "Optical spectroscopy of a surface at the nanometer scale: a theoretical study in real space," *Phys. Rev B* **49,** 11344 (1994).
31. C. Girard, A. Dereux, O. J. F. Martin, and M. Devel, "Importance of confined fields in near-field optical imaging of subwavelength objects," *Phys. Rev. B* **50,** 14467 (1994).
32. O. J. F. Martin, C. Girard, and A. Dereux, "Generalized field propagator for electromagnetic scattering and light confinement," *Phys. Rev. Lett.* **74,** 526 (1995).
33. W. E. Moerner and T. Basche, *Angew. Chem. Int. Ed. Engl.* **32,** 457 (1993).
34. M. Orrit and J. Bernard, "Single pentacene molecules detected by fluorescence excitation in a p-terphenyl crystal," *Phys. Rev. Lett.* **65,** 2716 (1990).
35. U. P. Wild, F. Guettler, M. Pirotta, and A. Renn, "Single molecule spectroscopy: stark effect of pentacene in p-terphenyl," *Chem. Phys. Lett.* **193,** 451 (1992).
36. M. Croci, H.-J. Müschenborn, F. Guettler, A. Renn, and U. P. Wild, "Single molecule spectroscopy: pressure effect of pentacene in p-terphenyl," *Chem. Phys. Lett.* **212,** 71 (1993).
37. F. Guettler, T. Irngartinger, T. Plakhotnik, A. Renn, and U. P. Wild, "Fluorescence microscopy of single molecules," *Chem. Phys. Lett.* **217,** 393 (1994).
38. W. E. Moerner, T. Plakhotnik, T. Irngartinger, U. P. Wild, D. W. Pohl, and B. Hecht, "Near-field optical spectroscopy of individual molecules in solids," *Phys. Rev. Lett.* **73,** 2764 (1994).

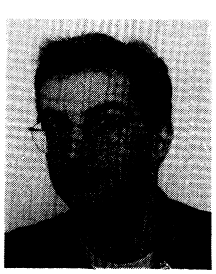

Harry Heinzelmann graduated from the University of Basel in 1986 and received his PhD degree in surface science and force microscopy in 1989. He spent 2 years at the IBM Almaden Research Center in San Jose, California, where he was involved in experiments to directly observe the motion of single molecules and in low-temperature tunneling microscopy. In 1992 he went to the IBM Zürich Research Center, where he began to work on near-field optical microscopy. He is now back at the University of Basel. His current research interests are microscopy and spectroscopy on the nanometer scale and further development and application of different near-field optical microscopy schemes toward this goal.

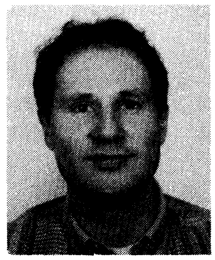

Thomas Huser graduated in physics from the University of Basel in 1994. His diploma thesis dealt with the construction of a scanning tunneling optical microscope. At present he is working toward a PhD. His present research concerns the improvement of scanning tunneling optical microscopy and the development of a reflection scanning near-field optical microscope that could be used for high-resolution Raman spectroscopy.

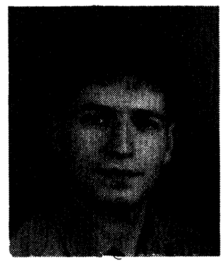

Thilo Lacoste studied physics at the Technical University of Darmstadt, where he did his diploma thesis on scanning force microscopy in 1994. He is now working toward his PhD in the scanning probe microscopy group of Prof. Güntherodt at the University of Basel. He is particularly interested in fluorescence and polarization contrast in scanning near-field optical microscopy.

Hans-Joachim Güntherodt received his PhD degree from the Swiss Federal Institute of Technology (ETH) in Zürich in 1967. His thesis was concerned with electronic transport in liquid metals. He remained at the ETH to continue his liquid metals research until 1974, when he joined the Institute of Physics in Basel as a full professor and head of the department. He was dean of the Faculty of Natural Sciences of the University of Basel in 1986 and 1987 and is currently rector of the university. His principal research interests are condensed matter physics: liquid metals, metallic glasses, rapidly quenched quasi- and nanocrystalline alloys, graphite intercalation compounds, electron spectroscopy, scanning probe microscopy, high-T_c superconductors, and fullerenes. He is coauthor of the books *Glassy Metals I, II and III* and of the books *Scanning Tunneling Microscopy I, II, and III* (Springer Publishers).

Dieter W. Pohl studied at the Universities of Stuttgart, Hamburg, and Munich, where he received his PhD in physics from the Technical University in 1968. Since, he has been a research staff member at the IBM Research Laboratory in Rüschlikon. From 1968 to 1979 he worked on laser physics and nonlinear optics. He then spent one year at the IBM T. J. Watson Research Center, Yorktown Heights, New York. Since 1982, his interest has been in scanning tunneling microscopy (STM) and related techniques, in particular, near-field optical microscopy. Pohl is author of about 120 papers and holds several patents on scanning probe microscopy, micromechanics, and storage. He received an award for introduction of STM to IBM technology in 1988.

Bert Hecht graduated with a degree in physics from the University of Konstanz in 1993. Hecht is currently a graduate student at the IBM Research Laboratory in Rüschlikon, where he is pursuing studies on novel schemes and instrumentation for near-field optics.

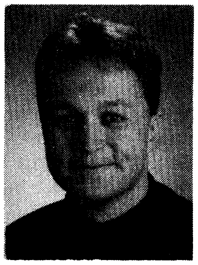

Lukas Novotny studied electrical engineering at the Swiss Federal Institute of Technology (ETH) in Zürich from 1986 to 1992. Since, he has been a graduate research assistant at the Laboratory for Field Theory and High Frequency Electronics at ETH in Zürich.

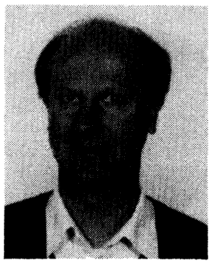

Olivier J. F. Martin received the Diplôme d'Ingénieur Physicien and the PhD degree in physics from the Swiss Federal Institute of Technology in Lausanne (EPFL), Switzerland, in 1989 and 1994, respectively. From 1989 to 1994 he was a PhD student at the IBM Research Laboratory in Rüschlikon, and in 1995 he joined the Swiss Federal Institute of Technology in Zürich, where he is currently a research scientist. His research interests include computational electromagnetics with an emphasis on integrated optics and on the calculation of optical fields in confined geometries.

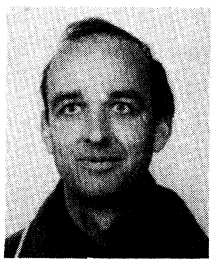

Christian V. Hafner received his diploma in 1975 and a PhD in electrical engineering in 1980 from the Swiss Federal Institute of Technology (ETH) in Zürich, where he is now a lecturer. Since 1980, he developed the generalized multipole technique (GMT) for computational electromagnetics and the multiple multipole method (MMP) code based on this technique. His current research focuses on the comparison, combination, and generalization of numerical methods and on historical and philosophical ideas of the theory of electromagnetism. He has published textbooks in German and English and two book/software packages.

Heinrich Baggenstos is a full professor of electrical engineering at the Swiss Federal Institute of Technology (ETH) in Zürich, where he received his diploma in 1956. His special interest is basic training and research in electrical engineering. Prof. Baggenstos leads research groups in computational electrodynamics, electromagnetic compatibility, and bioelectromagnetics.

Urs P. Wild is a full professor of physical chemistry at the Swiss Federal Institute of Technology (ETH) in Zürich. The focus of his research group is photochemistry and photophysics of molecules in amorphous materials and crystals at low temperatures. His special research topics are spectral hole burning, molecular computing, photography, femtosecond spectroscopy, and single-molecule spectroscopy. Wild has published more than 200 papers.

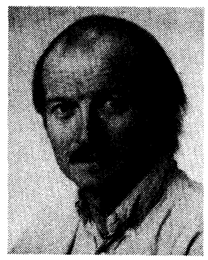

Alois Renn is U. P. Wild's coworker at the Swiss Federal Institute of Technology (ETH), Zürich. He received his PhD degree from the Technical University of Berlin in gas phase molecular spectroscopy. Since 1983 he has been at the ETH in Zürich. His main interest is laser spectroscopy of low-temperature solids with an emphasis on spectral hole burning and single-molecule spectroscopy. He published more than 50 papers in this field.